2022 Basin and Range Earthquake Summit (BRES)

Geology - Monday October 17

Session Conveners: Alex Hatem (U.S. Geological Survey), Rich Koehler (Nevada Bureau of Mines and Geology), and Zach Lifton (Idaho Geological Survey)

Invited speakers:

Jeri Ben-Horin	Arizona Geological Survey	Timing of Mead slope fault ruptures, Lake Mead area, Arizona
Seth Dee	Nevada Bureau of Mines and Geology	Geologic mapping, geochronology, and fault characterization in the Las Vegas Basin
Yann Gavillot	Montana Bureau of Mines and Geology	Late quaternary slip rates and surface rupture of the Bitterroot Fault, western Montana
Egill Hauksson	Caltech	The 2020 M_w55.8 Lone Pine, eastern California, normal-faulting earthquake sequence
Adam Hiscock	Utah Geological Survey	Geologic setting and geologic effects of the March 2020 M_w5.7 Magna, Utah, earthquake
Jessica Jobe	U.S. Geological Survey	Mapping of potentially active faults in the vicinity of the 2019 Ridgecrest earthquake ruptures, California
Rich Koehler	Nevada Bureau of Mines and Geology, University of Nevada, Reno	Field response and surface rupture characteristics of the 2020 M6.5 Monte Cristo Range earthquake, central Walker Lane, Nevada
Zach Lifton	Idaho Geological Survey	Tectonic background of the 2020 M_w6.5 Stanley, Idaho earthquake and a summary of current work
James Mauch	Wyoming State Geological Survey	Faults on the fringe: New mapping of discreet faults in northwest Wyoming
Lucy Piety	U.S. Bureau of Reclamation	Evidence for quaternary activity on the Deadwood-Reeves Creek Fault, west-central Idaho
Seth Wittke	Wyoming State Geological Survey	Paleoseismic investigation of the South Granite Mountains Fault, central Wyoming

TIMING OF MEAD SLOPE FAULT RUPTURES, LAKE MEAD AREA, ARIZONA

Jeri Young Ben-Horin, Arizona Geological Survey, jeribenhorin@arizona.edu
Brian F. Gootee, Arizona Geological Survey, bgootee@arizona.edu
Cassandra Fenton, Colorado Mesa University, cassiefenton@gmail.com
Greg Balco, Berkeley Geochronology Center, balcs@bgc.org
Jean Thomas Marso, Colorado Mesa University, c/o cassiefenton@gmail.com
Reno Davidson, Colorado Mesa University, c/o cassiefenton@gmail.com
Philip A. Pearthree, Arizona Geological Survey, pearthre@arizona.edu
Tammy Rittenour, Utah State University, tammy.rittenour@usu.edu

ABSTRACT

The Mead Slope fault (MSF) has been considered an active late Quaternary fault for several decades; however, until this study, there have been weak constraints on slip rates, and the age and size of surface-rupturing earthquakes. We used high-resolution DEMs, cosmogenic dating of alluvial fans, OSL dating of faulted sediments, and detailed examination of fault exposures to better constrain the earthquake histories for the main fault strand. Detailed fault mapping was accomplished using DEMs generated from multiple drone flights and ground-control points. We determined that the fault zone consists of two main strands, both offsetting Quaternary alluvial fan remnants. The northwestern strand offsets late to latest Pleistocene fan deposits, as well as relatively young tributary gravel deposits exposed below a wave-cut bench associated with past high levels of Lake Mead. Examination of this exposure revealed 2 or 3 identifiable surface ruptures that occurred within the past ~60,000 yrs. We collected 21 surface rock samples from various Quaternary landforms displaced by the fault for exposure dating via cosmogenic ^{3}He. Preliminary exposure dates from several alluvial fans provide age constraints for a long-term slip rate as well as a slip rate for the past 150 ky. Three samples were taken from large boulders exposed on the surface of a Qo alluvial fan resulting in preliminary exposure ages that range from 620 to 880 ka. Given the Qo landform has been left-laterally offset by at least 80m, the long-term slip rates for the northwestern most strand range from 0.09 to 0.13mm/yr. Three samples collected from large boulders on late Pleistocene fan units (Qi3-4) yielded preliminary ^{3}He exposure ages ranging from 80 to 147 ka. Left-lateral offsets on the Qi3-4 surfaces are approximately 5-6 m, with less than 2 m of vertical offset. This indicates a lateral slip rate of 0.03 to 0.06mm/yr since 150 ka. Given the fault exposure in the tributary sediments reveals at least 2 events since 60 ka and at least one older earthquake, it is likely that they are represented in the 5-6 m of offset of the Qi3-4 fan surfaces.

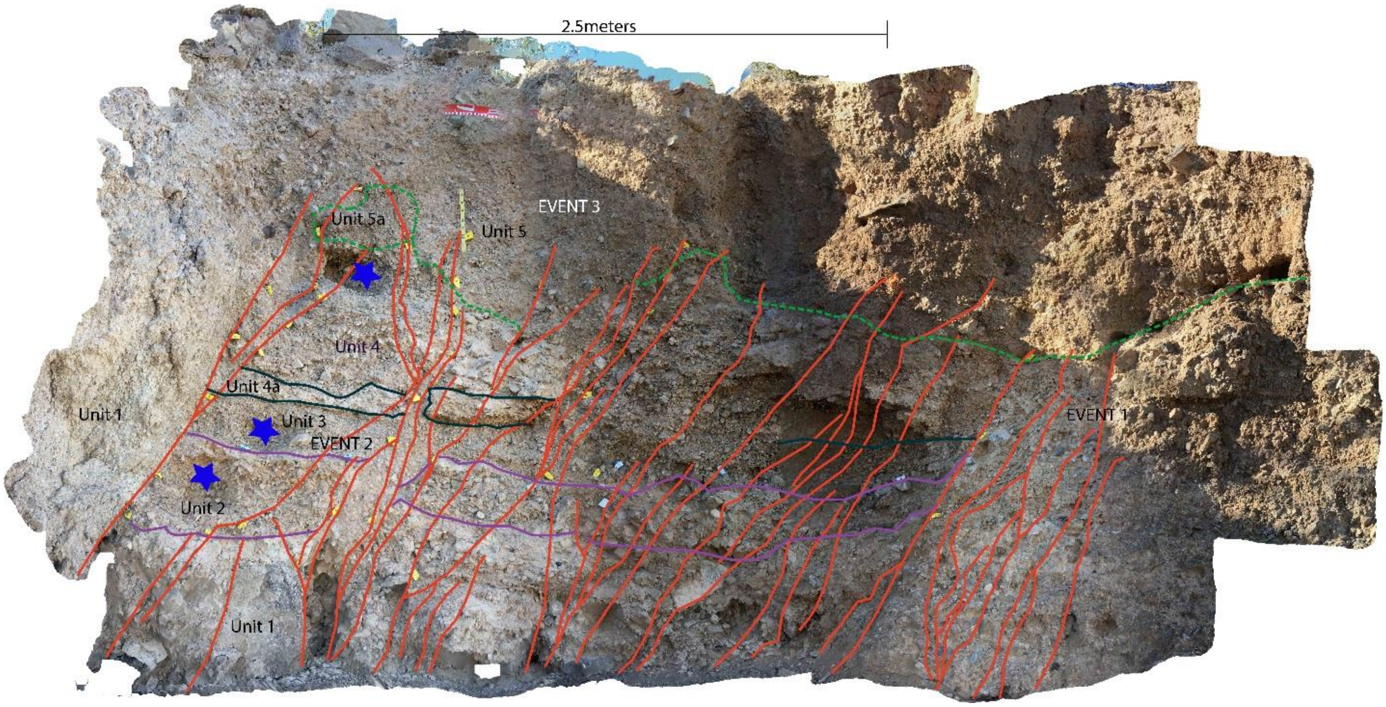

Figure 1. *Faulted tributary sediments exposed by Lake Mead lake level. Multiple strands shown as red line work, blue stars are OSL sample locations, units numbered in black. There are 2 to 3 events recorded in these sediments with one occurring in older gravels near the base of the wall, and on its west side (right side in photo) and one occurring after deposition of unit 2. There may be an additional event recorded in the uppermost portion of the exposure; View to the south.*

Geologic Mapping, Geochronology, and Fault Characterization in the Las Vegas Basin

Seth Dee, Nevada Bureau of Mines and Geology, University of Nevada, Reno, sdee@unr.edu
Craig M. dePolo, Nevada Bureau of Mines and Geology, University of Nevada, Reno, eq_dude@sbcglobal.net
Alan R. Ramelli, Nevada Bureau of Mines and Geology, University of Nevada, Reno, alanramelli@gmail.com
Shannon A. Mahan, U.S. Geological Survey, Geosciences and Environmental Change Science Center, smahan@usgs.gov
Wanda J. Taylor, University of Nevada Las Vegas, Department of Geoscience wanda.taylor@unlv.edu

A recent investigation into the seismic hazard of the Las Vegas basin includes a new surficial geology and Quaternary fault map, luminescence dating, and paleoseismic investigations of the Las Vegas Valley fault system (LVVFS) and Frenchman Mountain fault system (FMFS). The new 1:50,000 scale map involved the compilation of twenty published 1:24,000 scale maps and new geologic mapping. The compilation utilized historical aerial imagery, lidar, and a new orthophoto mosaic and DEM derived from 1965 aerial stereo photos. This new mapping improves the accuracy of Quaternary fault locations and yields a consistent characterization of surficial units displaced by the faults. The mapping was accompanied by 37 new luminescence ages to better constrain the age of offset stratigraphy. The luminescence data includes ages from the fine-grained ground water discharge deposits of the Las Vegas Formation (LVF) as well as alluvial fan deposits.

The LVVFS is a set of east-facing, northerly striking, intra-basin fault scarps up to 30 m high that displace LVF and alluvial fan deposits within the Las Vegas metropolitan area. Two paleoseismic trenches were excavated across the Eglington-Decatur fault, the westernmost in the LVVFS and the only fault with a continuous section of undeveloped scarps. The trenches exposed broadly warped LVF stratigraphy with 4-5 m of displacement and no evidence for brittle faulting. Luminescence and radiocarbon ages constrain the age of warp formation as occurring between ~27 and ~8 ka, with no displacement for the preceding ~300,000 years. Preliminary displacement rates derived from the trench results have significant temporal variability, a shorter-term rate of ~0.15 –0.18 mm/yr and a maximum longer-term rate of ~0.03 mm/yr.

The FMFS is an arcuate, west-dipping, range-bounding normal and dextral-oblique fault on the eastern side of the Las Vegas basin. The entire length of the FMFS was remapped during this investigation utilizing lidar data and the pre-development orthophoto mosaic. The new mapping identified scarps along a southern section of the fault that displace an alluvial fan surface of probable late-Pleistocene, and adjacent fault kinematics documenting dextral-oblique slip. These observations confirm a component of dextral slip along the southern FMFS and extends the total fault length with evidence for Quaternary displacement to ~33 km. We also conducted a paleoseismic investigation of a previously excavated fault exposure in a late-Pleistocene alluvial fan along the northern section of the FMFS. Logging of the excavation documents evidence for three paleoearthquakes with luminescence ages from colluvial wedge deposits ranging from ~54 to ~25 ka. Scarp profiling conducted during previous investigations prior to widespread development coupled with new luminescence ages from displaced deposits yield a preliminary, vertical slip rate estimate of 0.11-0.20 mm/yr.

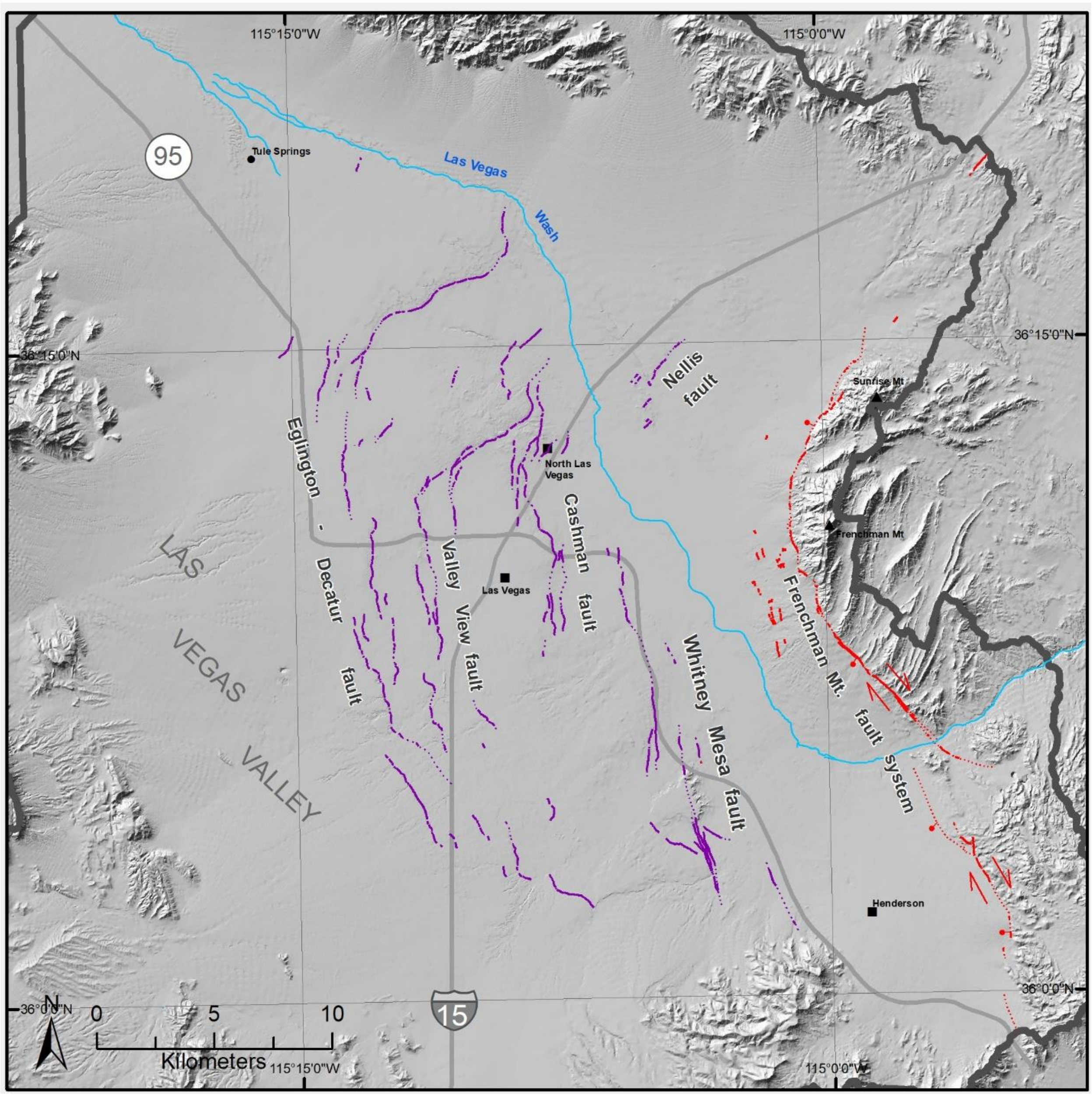

Quaternary faults of the Las Vegas Valley. Faults dotted where concealed or inferred. The Las Vegas Valley fault system, shown in purple, includes the Eglington - Decatur, Valley View, Cashman, Nellis and Whitney Mesa faults. Other faults including the Frenchman Mountain fault system are shown in red with bar and ball symbol showing the downthrown side of fault and arrows showing dextral oblique sections.

Late Quaternary Slip Rates and Surface Rupture of the Bitterroot Fault, Western Montana

Yann Gavillot[1], Jeffrey Lonn[1], Michael Stickney[1], Alan Hidy[2,]

[1]Montana Bureau of Mines and Geology, Montana Technological University
1300 W. Park Street, Butte, MT 59701
[2]Center for Accelerator Mass Spectrometry, Lawrence Livermore National Laboratory
7000 East Avenue, Livermore, CA 94550

ABSTRACT

The Bitterroot fault is a 100-km-long active normal fault that bounds the eastern margin of the north-south trending Bitterroot Mountains and accommodates extension within the Intermountain Seismic Belt. Earthquake and fault history are unknown for the Bitterroot fault, although the seismic risk is potentially high given the proximity of the rapidly growing towns in the Missoula–Bitterroot valleys. New detailed mapping using LiDAR along the southern Bitterroot Range documents multiple generations of fault scarps in Holocene-Pleistocene deposits with vertical offsets that increase in magnitude with age. Fault mapping indicates a complex fault geometry characterized by an *en echelon* pattern of discontinuous segments of 45–70° east-dipping normal faults that appear to cut the older Eocene detachment fault, and locally 70–80° west-dipping antithetic normal faults. ^{10}Be cosmogenic radionuclides surface exposure dating technique provides age control for 32 boulders sampled in glacial deposits. Near Como Dam, a dated 16–17 ka Pinedale moraine offset by the Bitterroot fault scarp with a vertical separation of 3.5 ± 0.1 m, yields a fault slip rate of 0.2–0.3 mm/yr. Glacial Lake Missoula shorelines inset into a dated ~15 ka Pinedale moraine and vertically offset 4.6 ± 1.5 m by an antithetic strand of the Bitterroot fault, yield fault slip rates of 0.2–0.4 mm/yr. In the Ward Creek Fan located ~15 km to the north of Como Dam, two dated ~17 ka and 63–70 ka fan surfaces offset by the Bitterroot fault with vertical separations of 2.4 ± 0.2 m and 4.5 ± 0.1 m, yield fault slip rates of 0.1–0.2 mm/yr and 0.1 mm/yr, respectively. Our results indicate broadly consistent fault slip rates with an along-strike preferred average of 0.2–0.3 mm/yr for the southern Bitterroot fault. Fault scaling relations, structural model constraints and our slip rate results indicate both a seismogenic low angle and high angle fault geometry are possible at depth, which could generate a M_w ~7.2 earthquake or larger. We speculate the Bitterroot fault is likely characterized by a millennia-timescale earthquake recurrence interval. Forthcoming paleoseismic trench results on the Bitterroot fault will aim to develop a Holocene-Pleistocene paleoearthquake chronology. Data from this study suggest seismic hazards from the Bitterroot fault potentially pose a significant risk to the Missoula metropolitan area, the State's second most populous region, and major infrastructures across the Missoula-Bitterroot valleys.

THE 2020 Mw5.8 LONE PINE, EASTERN CALIFORNIA, NORMAL-FAULTING EARTHQUAKE SEQUENCE

Egill Hauksson, California Institute of Technology, hauksson@caltech,edu
Brian Olson, California Geological Survey, brian.olson@conservation.ca.gov

ABSTRACT

The 2020 M_w 5.8 Lone Pine earthquake, the largest earthquake on the Owens Valley fault zone, eastern California, since the 19th century, ruptured an extensional step over in that fault. Owens Valley separates two normal faulting regimes, the western margin of the Great Basin and the eastern margin of the Sierra Nevada, forming a complex seismotectonic zone, and a possible nascent plate boundary. Foreshocks began on 22 June 2020; the largest M_w 4.7 foreshock occurred at ~6 km depth, with primarily normal faulting, followed ~40 hours later on 24 June 2020 by a M_w 5.8 mainshock at ~7 km depth. The sequence caused overlapping ruptures across a ~0.25 km^2 area, extended to ~4 km^2, and culminated in a ~25 km^2 aftershock area. The mainshock was predominantly normal faulting, with a strike of 330° (north-northwest), dipping 60° to 65° to the east-northeast. Comparison of background seismicity and 2020 Ridgecrest aftershock rates showed that this earthquake was not an aftershock of the Ridgecrest mainshock. The M_w-m_B relationship and distribution of ground motions suggest typical rupture speeds. The aftershocks form a NNW-trending, NNE dipping, 5 km long distribution, consistent with the rupture length estimated from analysis of regional waveform data. No surface rupture was reported along the 1872 scarps from the 2020 M_w 5.8 mainshock although the dipping rupture zone of the M_w 5.8 mainshock projects to the surface in the general area. The mainshock seismic energy triggered rock falls at high elevations (>3.0 km) in the Sierra Nevada at distances of 8 to 20 km, and liquefaction along the western edge of Owens Lake. Because there were ~30% fewer aftershocks than for an average southern California sequence, the aftershock forecast probabilities were lower than expected. ShakeAlert, the earthquake early warning system, provided first warning within 9.9 s, as well as subsequent updates.

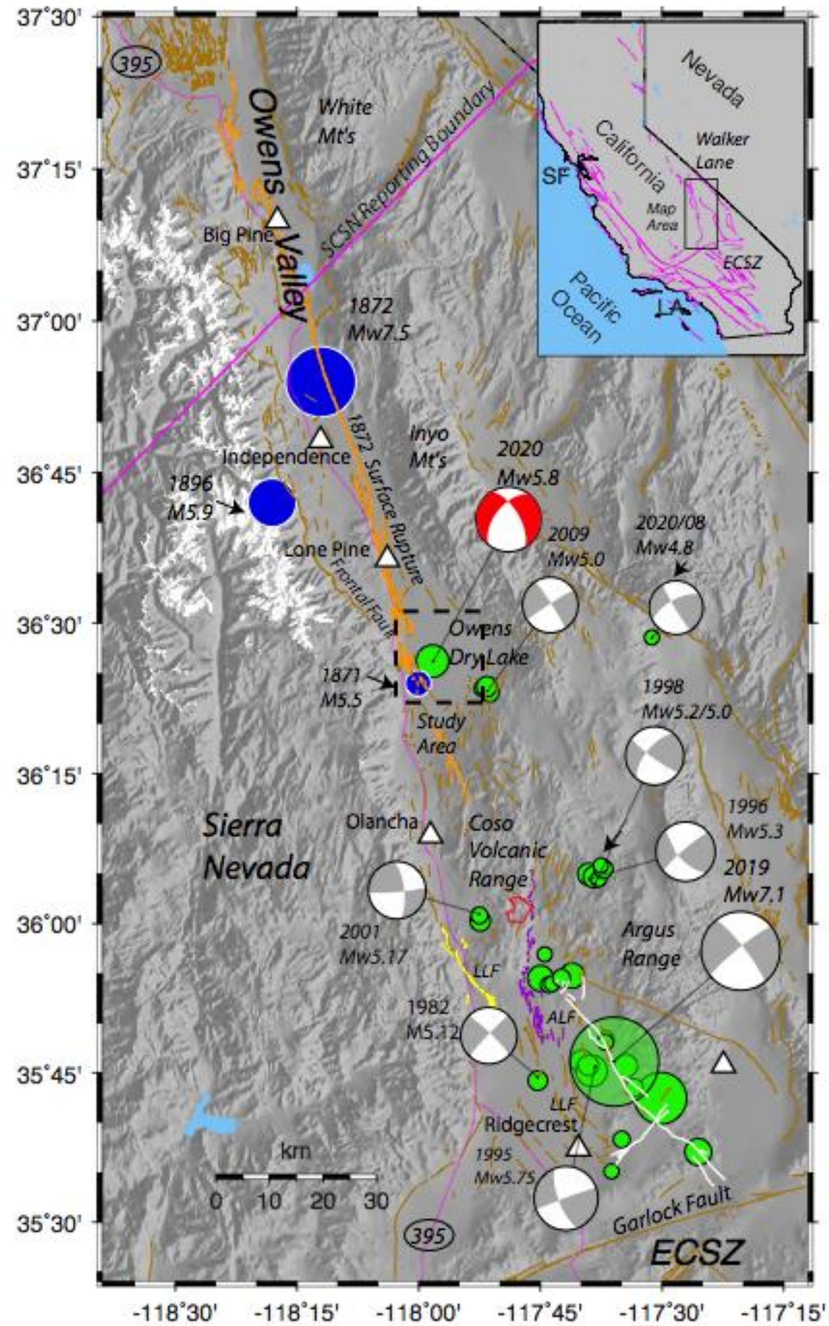

Figure 1. *Map of Owens Valley and adjacent regions in eastern California. Major earthquakes that occurred in the late 19th century are shown as labelled blue dots scaled with magnitude (Felzer and Cao, 2008; Ellsworth, 1990). Location of this map is shown in upper-right corner. Late Quaternary faults from Jennings and Bryant (2010) are shown in brown. The 1872 Mw 7.5 surface rupture is shown in orange (Haddon et al., 2016). Seismicity of M≥5 since 1980 is shown as green dots scaled with magnitude, with lower hemisphere focal mechanisms shown for significant events. The focal mechanism of the 2020 Mw 5.8 Lone Pine earthquake is shown in red. The 2020 August Mw 4.8 Stovepipe Wells earthquake is also included for reference. The detailed study area that is shown in later figures is outlined with dashed black lines. The SCSN northern reporting boundary is shown in magenta. ECSZ - eastern California shear zone. The US (395) highway is shown as a curvy magenta line and local towns are marked as triangles (From: Hauksson et al., 2021).*

GEOLOGIC SETTING AND GEOLOGIC EFFECTS OF THE MARCH 2020 M_W 5.7 MAGNA, UTAH, EARTHQUAKE

Adam I. Hiscock, Utah Geological Survey, adamhiscock@utah.gov
Adam P. McKean, Utah Geological Survey, adammckean@utah.gov
Emily J. Kleber, Utah Geological Survey, emilykleber@utah.gov
Michael D. Hylland, Utah Geological Survey, mikehylland@utah.gov
Christian L. Hardwick, Utah Geological Survey, christianhardwick@utah.gov
Greg N. McDonald, Utah Geological Survey, gregmcdonald@utah.gov
Zachary W. Anderson, Utah Geological Survey, zanderson@utah.gov
Grant C. Willis, Utah Geological Survey, grantwillis@utah.gov
Steve D. Bowman, Utah Geological Survey, stevebowman@utah.gov
Ben A. Erickson, Utah Geological Survey, benerickson@utah.gov

ABSTRACT

The March 18, 2020, M_w 5.7 Magna earthquake was the largest earthquake in Utah since the 1992 M_L 5.8 St. George earthquake. This normal-faulting earthquake occurred in the northwest corner of the Salt Lake Valley, home to 1.2 million people. The geologic setting of the Magna earthquake is well documented by recent geologic mapping and geophysical data in the Salt Lake Valley, in addition to seismicity data from the mainshock and aftershock sequence. Based on these data, we believe the mainshock of the Magna earthquake occurred on a relatively gently dipping part of the Salt Lake City segment of the Wasatch fault zone, with aftershocks concentrated on the West Valley fault zone and other subsidiary faults. Post-earthquake rapid reconnaissance teams organized by the Utah Geological Survey documented geologic effects using a small, unmanned aircraft system (sUAS) to obtain aerial photos and videos to supplement ground-based observations. Observed geologic effects include liquefaction in the form of sand boils, tension cracks, lateral spreading, and localized subsidence near the earthquake epicenter, along the Jordan River, and along the shoreline of the Great Salt Lake. Potential syneresis cracking and pooling in large areas indicated fluctuating groundwater likely related to earthquake ground shaking. No primary surface fault rupture was observed. A web-based digital clearinghouse was established to collect, distribute, and archive data related to the earthquake (https://geodata.geology.utah.gov/pages/search.php?search=!collection609). Ground shaking caused at least $70 million in public infrastructure damage in Salt Lake and Tooele Counties, with additional damage to residential and commercial properties. The moderate magnitude, associated geologic effects, and infrastructure damage values from the Magna earthquake highlight the critical importance of earthquake research from multidisciplinary fields in the geosciences and preparedness along the Wasatch Front.

MAPPING OF POTENTIALLY ACTIVE FAULTS IN THE VICINITY OF THE 2019 RIDGECREST EARTHQUAKE RUPTURES, CALIFORNIA

Jessica Thompson Jobe, U.S. Geological Survey, jjobe@usgs.gov
Belle Philibosian, U.S. Geological Survey, bphilibosian@usgs.gov
Colin Chupik, Bureau of Reclamation, cchupik@usbr.gov
Judith Zachariasen, California Geological Survey, judith.zachariasen@conservation.ca.gov
Timothy Dawson, California Geological Survey, timothy.dawson@conservation.ca.gov
Carla Rosa, California Geological Survey, carla.rosa@conservation.ca.gov

ABSTRACT

The region near the July 2019 Ridgecrest earthquake sequence in southeastern California had not been comprehensively examined for active faults prior to those earthquakes. No long continuous faults or fault zones spanning the entire rupture had been recognized in the area, and only ~35% of the rupture occurred on previously mapped faults (Figure 1). Using pre-event high-resolution (<2 m) topography and optical imagery, in combination with post-event field observations and unmanned aerial vehicle imagery, we document geomorphic evidence of pre-2019 faulting along both the Paxton Ranch (M7.1 surface rupture) and Salt Wells Valley (M6.4 surface rupture) fault zones. These fault-related features include tufa lineaments, sheared Quaternary deposits, scarps, deflected drainages, and topographic, vegetation, and ground color lineaments and contrasts. These features reveal a network of orthogonal northeast- and northwest-striking fault traces, a subset of which ruptured in 2019. Neotectonic features are commonly short (<2 km), discontinuous, and display left-stepping en echelon patterns along both the M6.4 and M7.1 surface ruptures. Faults are generally better expressed and preserved outside the late Pleistocene lake basins and in areas where substantial vertical motion occurred in 2019. Both the northeast- and northwest-striking active fault systems are subparallel to regional bedrock fabrics that were established as early as ~150 Ma. These fault systems may be reactivating older structures subparallel to the bedrock fabric. The newly identified faults recognized in the pre-event data are being integrated with new mapping on post-earthquake high-resolution lidar data to develop an updated Quaternary fault map for the region.

Overall, we estimate that 50–70% of the 2019 surface ruptures could have been recognized as active faults with detailed inspection of pre-earthquake data. Similar detailed mapping of potential neotectonic features could help improve seismic hazard analyses in other regions of the Walker Lane – Eastern California Shear Zone, and elsewhere where there are distributed or incompletely mapped faults. To characterize regions of distributed faulting in seismic hazard analyses in areas where faults cannot be resolved as discrete throughgoing structures, we recommend using polygons that represents zones of potentially active faults, with slip distributed throughout the polygons.

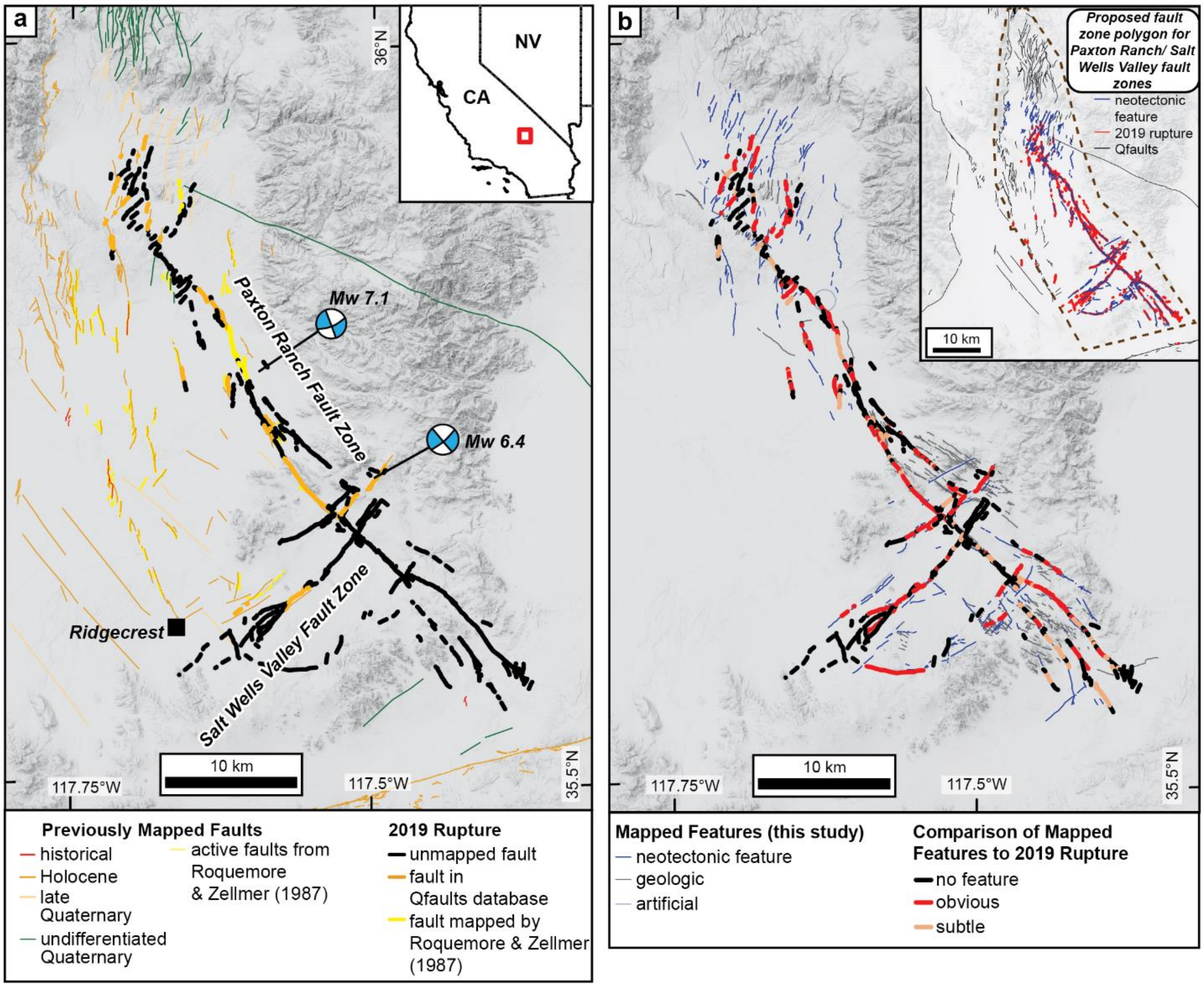

Figure 1. *(a) Comparison of the 2019 ruptures to previously mapped faults from the Quaternary fault and fold database/California fault activity map (Qfaults) and Roquemore and Zellmer (1987). Approximately 35% of the 2019 surface ruptures were on previously mapped faults. Inset shows location of Ridgecrest area in southern California. (b) Comparison of the 2019 surface rupture to the newly mapped neotectonic features from pre-earthquake data (gray lines represent geologic features, such as shorelines or dikes; light blue lines represent artificial features, which are likely anthropogenic in origin but appear as lineaments within the vicinity of the 2019 ruptures). Approximately 70% of the 2019 rupture occurred along pre-existing neotectonic features (red lines where neotectonic features were obvious; pink lines where neotectonic features were subtle and may not have been recognized prior to the 2019 events; black lines where no neotectonic features were observed along the 2019 surface rupture). Inset shows proposed fault zone polygon (brown dashed lines) for the Paxton Ranch and Salt Wells Valley fault zones, based on existing Qfaults, the 2019 rupture, and the neotectonic features. Figure modified from Thompson Jobe et al., 2020.*

FIELD RESPONSE AND SURFACE-RUPTURE CHARACTERISTICS OF THE 2020 M6.5 MONTE CRISTO RANGE EARTHQUAKE, CENTRAL WALKER LANE, NEVADA

Rich D. Koehler, Nevada Bureau of Mines and Geology, University of Nevada, Reno, rkoehler@unr.edu
Seth Dee, Nevada Bureau of Mines and Geology, University of Nevada, Reno, sdee@unr.edu
Austin Elliott, U.S. Geological Survey, Moffett Field, CA, ajelliott@usgs.gov
Alexandra Hatem, U.S. Geological Survey, Golden, CO, ahatem@usgs.gov
Alexandra Pickering, U.S. Geological Survey, Moffett Field, CA, Alijacqueline@gmail.com
Ian Pierce, Department of Earth Sciences, University of Oxford, Oxford, UK, ian.pierce@earth.ox.ac.uk
Gordon Seitz, California Geological Survey, San Mateo, CA, Gordon.Seitz@conservation.ca.gov

ABSTRACT

The M 6.5 Monte Cristo Range earthquake that occurred in the central Walker Lane on 15 May 2020 was the largest earthquake in Nevada in 66 yr and resulted in a multidisciplinary scientific field response. The earthquake was the result of left-lateral slip along largely unmapped parts of the Candelaria fault, one of a series of east–northeast-striking faults that comprise the Mina Deflection, a major right step in the north–northwest structural grain of the central Walker Lane. We describe the characteristics of the surface rupture and document distinct differences in the style and orientation of fractures produced along the 28 km long rupture zone. Along the western part of the rupture, left-lateral and extensional displacements occurred along northeasterly and north-striking planes that splay off the eastern termination of the mapped Candelaria fault (Figure 1). To the east, extensional and right-lateral displacements occurred along predominantly north striking planes that project toward well-defined Quaternary and bedrock faults. Although the largest left-lateral displacement observed was ∼20 cm, the majority of displacements were < 5 cm and were distributed across broad zones up to 800 m wide, which are not likely to be preserved in the geologic record. The complex pattern of surface rupture is consistent with a network of faults defined in the shallow subsurface by aftershock seismicity and suggests that slip partitioning between east-striking left-lateral faults and north to northwest-striking right-lateral faults plays an important role in accommodating northwest-directed transtension in the central Walker Lane. Prominent tectonic geomorphology along the unruptured western Candelaria fault (west of the 2020 surface rupture) including linear side-hill benches and troughs and left-laterally displaced channels suggests that potentially larger earthquakes are possible in the Mina Deflection.

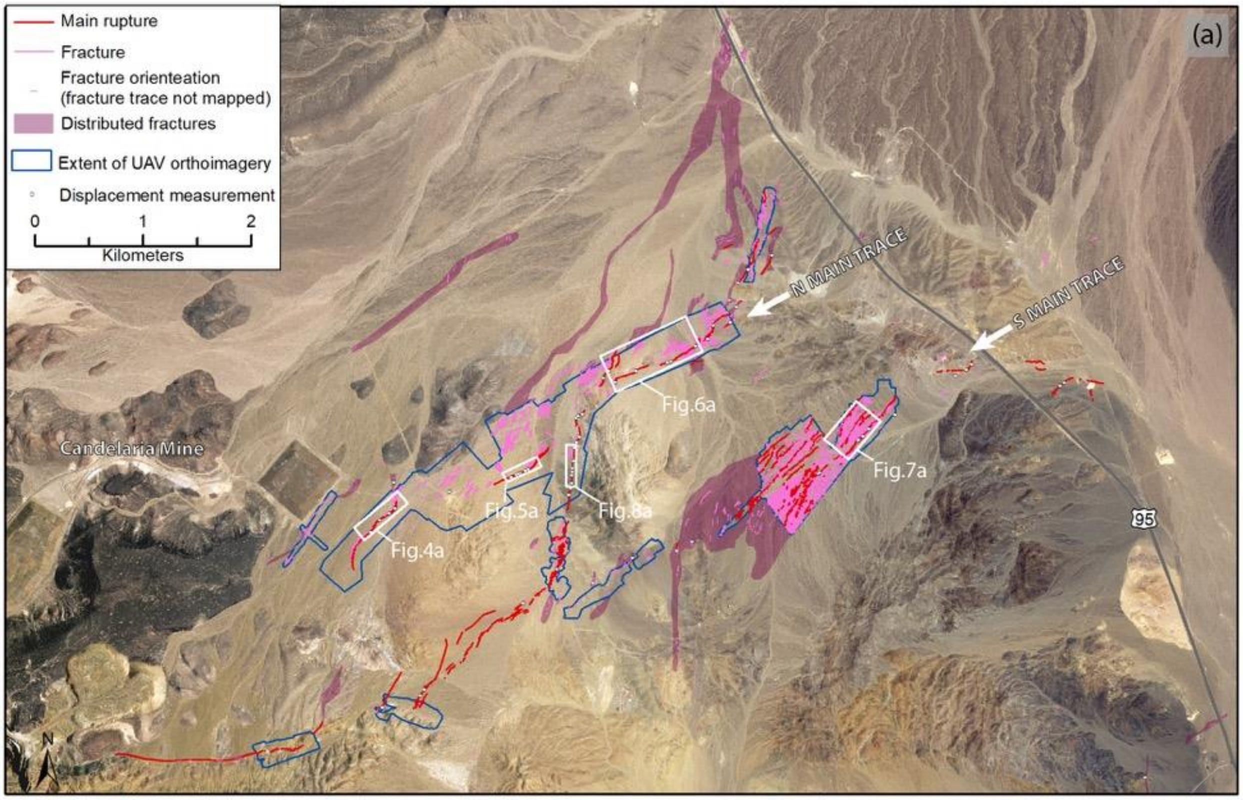

Figure 1. *Mapping results from the western part of the Monte Cristo Range earthquake surface-rupture showing main ruptures, fractures, and wide zones of distributed fracturing (Koehler et al., 2021; Dee et al., 2021).*

TECTONIC BACKGROUND OF THE 2020 M_W6.5 STANLEY, IDAHO EARTHQUAKE AND A SUMMARY OF CURRENT WORK

Zachery M. Lifton, Idaho Geological Survey, zlifton@uidaho.edu

ABSTRACT

The moment magnitude (M_w) 6.5 earthquake that occurred March 31, 2020, near Stanley, Idaho was felt widely across the western U.S., yet it caused only minor damage due to its remote location. No evidence has been found of surface rupture related to the earthquake, but InSAR interferograms show broad surface deformation of several centimeters. Secondary effects such as rockfall, snow avalanches, and liquefaction were observed throughout the epicentral region. The area is remote and sparsely instrumented, with the closest station to the mainshock approximately 100 km away. A robust, ongoing aftershock sequence has been recorded by a temporary network of 15 broadband seismometers and 24 nodal sensors.

The epicenter of the 2020 M_w6.5 Stanley earthquake was located within the granitic Idaho Batholith in central Idaho at the northern boundary of the Basin and Range Province. The segment of the Basin and Range Province north of the Snake River Plain, which includes the Sawtooth, Lost River, Lemhi, and Beaverhead faults, is part of the seismically active Centennial Tectonic Belt. The northern end of the Sawtooth fault is bound by the northeast-striking Trans-Challis fault system, a zone of Eocene age normal faults that are no longer active, but which may influence modern seismicity. Several moderate historical earthquakes have struck the 2020 epicentral area, including a M_s6.1 event in 1944 and a M_s6.0 event in 1945.

One of the biggest questions arising from this event is the location and geometry of the source fault. While the east-dipping Sawtooth normal fault would be an obvious source for an earthquake at this location, the mainshock was located north of the mapped trace of the Sawtooth fault and the focal mechanism suggested left-lateral strike-slip motion on a north striking fault. Aftershocks plot on a plane steeply dipping to the west. Several researchers are analyzing the earthquake and aftershock sequence to understand the rupture mechanism and fault geometry. The emerging picture is of a complex rupture, not on the Sawtooth fault but on one or more unmapped faults. Current work focuses on mapping surficial fault scarps with new lidar, dating key landforms to constrain the timing of past surface rupturing earthquakes, and attempting to excavate paleoseismic trenches.

FAULTS ON THE FRINGE: NEW MAPPING OF DISCREET FAULTS IN NORTHWEST WYOMING

James P. Mauch, Wyoming State Geological Survey, james.mauch@wyo.gov
Seth J. Wittke, Wyoming State Geological Survey, seth.wittke@wyo.gov
Nolan C. Barrette, Wyoming State Geological Survey contractor (now with U.S. Geological Survey), nbarrette@usgs.gov

ABSTRACT

Active normal faults in the Greater Yellowstone region reflect the influence of uplift associated with the Yellowstone hotspot superimposed on Basin and Range lithospheric extension. Along the northeast (leading) edge of the hotspot track are inconspicuous and enigmatic faults believed to be in an early stage of development. Because these faults lack the topographic signature of longer-lived range-bounding structures their detection is difficult, and they remain lightly studied. We present detailed mapping and scarp profile measurements of several such faults in easternmost Jackson Hole, Wyoming, which displace Pinedale-1 (~20 ka) and Pinedale-2 (~15 ka) glacial till and other Quaternary deposits.

The proposed Uhl Hill fault is a 4.5-km-long, southeast-dipping normal fault in eastern Grand Teton National Park with newly recognized Quaternary activity. Scarps in Pinedale-1 moraines have vertical surface offset (VSO) values two-to-three times greater than scarps in Pinedale-2 moraines, suggesting post-15 ka displacement and the possibility of multiple surface rupturing events from 20–15 ka. The Uhl Hill fault is expressed at its southern end by a 1-m-high scarp across part of the Spread Creek alluvial fan. A 1.5 km-long scarp in Pinedale-1 till ~4 km to the northeast across the Buffalo Fork valley may be a northern extension of the fault. 20 km east, the Togwotee Lodge faults form a complex system of sharp, east-facing, en echelon scarps in Bull Lake till (~150 ka), Pinedale-1 till, and colluvium. Scarps in Pinedale-1 till have highly variable VSO values with some of the largest measurements occurring near the northern terminus of the mapped fault system, suggesting a greater fault length than currently recognized. Field observations of scarps beyond the mapped extent are difficult due to obstruction by landslides and dense forest cover, and mapping of the Togwotee Lodge faults should be revisited once LiDAR data become available.

Our work highlights the need for future paleoseismic studies on these faults to answer unresolved questions of rupture timing, relation to regional structures like the Teton fault, and seismic hazard from other incipient faults in the Greater Yellowstone region.

EVIDENCE FOR QUATERNARY ACTIVITY ON THE DEADWOOD-REEVES CREEK FAULT, WEST-CENTRAL IDAHO

Julia C. Howe, Bureau of Reclamation, jhowe@usbr.gov
Lucille A. Piety, Bureau of Reclamation, lpiety@usbr.gov
Zachery M. Lifton, Idaho State Geological Survey, zlifton@uidaho.edu
Lee M. Liberty, Boise State University, lliberty@boisestate.edu

ABSTRACT

The Deadwood-Reeves Creek fault is a north-striking fault in the Idaho batholith. Its interpretation as Quaternary-active has been debated, and the fault is generally poorly understood. Uncertainties in its mapped location, style of deformation, and recency of activity stem largely from a complex geologic setting characterized by plutonic rock and a landscape altered by multiple Pleistocene glaciations. There is limited stratigraphy from which to measure long-term fault displacement, and Quaternary deposits are limited in extent, creating a challenging setting in which to assess Quaternary activity. Dense vegetation and steep terrain have also historically complicated evaluation based on aerial imagery and field reconnaissance. Although the Deadwood-Reeves Creek fault has previously been interpreted as a normal fault, its structure and topographic expression are distinctive from Basin and Range style normal faults to the east and west. It is steeply dipping and characterized by linear, incised glacial valleys in mountainous terrain, with basins located at bends in the mapped traces. These characteristics suggest that the Deadwood-Reeves Creek fault may be strike-slip or oblique.

Lidar encompassing the fault reveals previously unmapped fault scarps, the most prominent of which are within Deadwood basin. In 2021, we excavated a trench across a scarp at the northern end of Deadwood basin near Habit Creek. The Habit Creek scarp crosses a high surface, an inset alluvial surface, and beheads several southeast-flowing drainages. Vertical separations range from ~2.6-4.9 m across the high surface and ~0.34 m across the alluvial surface. The Habit Creek scarp is antithetic to the primary basin-bounding fault and has not previously been mapped as a fault trace. A seismic reflection profile at the trench location shows clearly offset reflectors to a depth of at least 80 m. At depths shallower than ~50 m, there is a complex zone of offset and deformation up to ~60 m wide. The trench was excavated across the primary offset reflector corresponding to the geomorphic scarp, exposing glaciolacustrine deposits in fault contact with fine grained sediment at the base of the scarp. Minor displacements of the fine sediment persist away from the primary fault, consistent with a broad zone of deformation. Work to refine the activity rate of the Deadwood-Reeves Creek fault is ongoing.

PALEOSEISMIC INVESTIGATION OF THE SOUTH GRANITE MOUNTAINS FAULT, CENTRAL WYOMING

Sylvia R. Nicovich, Bureau of Reclamation, snicovich@usbr.gov
Colin M. Chupik, Bureau of Reclamation, cchupik@usbr.gov
Ralph E. Klinger, Bureau of Reclamation, rklinger@usbr.gov
Seth J. Wittke, Wyoming Geological Survey, seth.wittke@wyo.gov
Harrison J. Gray, United States Geological Survey, hgray@usgs.gov

ABSTRACT

The northwest trending, 135-km-long South Granite Mountains fault (SGMF) is a significant contributor to the seismic hazard at multiple Bureau of Reclamation (BOR) facilities along the North Platte River in central Wyoming. The SGMF bounds the northern extent of the Seminoe and Ferris Mountains, Green Mountain, and Crooks Mountain. Evidence of the down-to-the-north, high-angle fault system consists of linear but discontinuous fault scarps, vegetation lineaments and springs, apparent offset drainages, hillside benches, and topographic slope breaks. The SGMF is divided into five major segments. From east to west these are the Seminoe Mountains, Ferris Mountains, Muddy Gap, Green Mountain, and Crooks Mountain segments. To better characterize the SGMF for hazard analysis, we excavated three paleoseismic trenches along the two most proximal segments to BOR facilities; two trenches along the Seminoe Mountains segment, and one along the Ferris Mountains segment. Previous paleoseismic studies have recognized only the Ferris Mountains and Green Mountain segments to have late Quaternary activity. Our data show possible Quaternary faulting on the Seminoe Mountains segment and supporting evidence for late Pleistocene and early Holocene ground rupturing earthquakes on the Ferris Mountain segment.

Geology - Monday October 17

Session Conveners: Alex Hatem (U.S. Geological Survey), Rich Koehler (Nevada Bureau of Mines and Geology), and Zach Lifton (Idaho Geological Survey)

Poster Session:

Christopher DuRoss	U.S. Geological Survey	Are Wasatch Front earthquakes preserved in the Great Salt Lake sedimentary record?
Austin Elliott	U.S. Geological Survey Earthquake Science Center	Rupture in the Mina Deflection: Activation of the full range of transtensional faults during the 2020 Monte Cristo Range earthquake sequence
Alex Hatem	U.S. Geological Survey	Preliminary analysis of earthquake geology input data for the U.S. National Seismic Hazard Model 2023 update
Suzanne Hecker	U.S. Geological Survey	Geologic evidence of earthquake behavior on the eastern edge of the Basin and Range
Tyler Knudsen	Utah Geological Survey	Detailed quaternary fault-trace mapping of the Washington, Hurricane, and Sevier Toroweap Fault Zones in Utah and Arizona
Rich Koehler	Nevada Bureau of Mines and Geology, University of Nevada, Reno	Quaternary fault compilation for the INGENIOUS geothermal project
Charles Memmott	Utah Valley University	Insights into segmentation of the Oquirrh-Great Salt Lake Fault system from fault scarp heights and Lake Bonneville shoreline elevations
Kristen E. Smith	Utah Valley University	Paleoseismic History of the Genola North Fault at the West Mountain Site and connectivity with Utah Lake Faults
Nathan A. Toké	Utah Valley University	Lidar data reveal evidence for late quaternary faulting 5km east and nearly 1000 m above the Bonneville High Stand, cutting glacial moraines and talus cones of the Timpanogos massif along the northern Provo segment of the Wasatch Fault
Mark Zellman	BGC Engineering	Lidar data reveal new faults in the epicentral region of the 2020 M6.5 Stanley, Idaho earthquake

ARE WASATCH FRONT EARTHQUAKES PRESERVED IN THE GREAT SALT LAKE SEDIMENTARY RECORD?

Christopher B. DuRoss, U.S. Geological Survey, cduross@usgs.gov
Daniel S. Brothers, U.S. Geological Survey, dbrothers@usgs.gov
Jessica A. Thompson Jobe, U.S. Geological Survey, jjobe@usgs.gov
Drake M. Singleton, U.S. Geological Survey, dsingleton@usgs.gov
Amanda Rossi, University of Wyoming, arossi2@uwyo.edu

ABSTRACT

Lacustrine paleoseismology, including interpretations from seismic stratigraphy and sediment cores, can yield high-fidelity records of earthquake timing, recurrence, and shaking intensity. Here, we apply these methods to the Great Salt Lake, Utah (GSL; Figure 1) to address questions such as: (1) Are sedimentological records of earthquakes (e.g., mass-transport deposits) present in the GSL record? (2) If so, can on-fault (e.g., Great Salt Lake fault zone) and off-fault (e.g., Wasatch fault zone) earthquake records be differentiated? (3) Did the 2020 M5.7 Magna earthquake (Figure 1) disturb GSL sediments? Our goal is to build on previous work demonstrating as many as six Holocene Great Salt Lake fault earthquakes (Dinter and Pechmann, 2005), compare our results to Wasatch fault zone trench data, and provide an additional, independent record of prehistoric strong shaking along the northern Wasatch Front.

Our study is focused on the south arm of the GSL, along the western shore of Antelope Island (Figure 1). In June–July 2021, we collected 420 line-km of subbottom Chirp data, which image the uppermost 20–30 m of unconsolidated lake sediment at 12–15 cm resolution. Guided by interpretations of faulting and related unconformities, we extracted 38 mini hammer cores, which are 6 cm in diameter, 81–189 cm in length, and represent several thousand years of sediment accumulation depending on the site. X-ray computed tomography (CT) density scans and photo logs of the cores reveal finely laminated brine-shrimp fecal pellet silt to fine sand. Along the base of the Great Salt Lake sublacustrine fault scarp near Antelope Island (Figure 1c), the laminated sediments in some cores are truncated by massive, ≤20-cm thick, normally graded beds. These beds may represent sediment disruption and/or transport during past earthquake shaking. We plan to (1) use the Chirp imagery to examine evidence of Great Salt Lake faulting, stratigraphic growth, and earthquake-related unconformities; (2) document the core sedimentology and relate possible earthquake disturbance horizons to the seismic stratigraphy and historical shaking events such as the Magna earthquake; and (3) evaluate Bayesian models of earthquake timing using charcoal and brine shrimp cysts extracted for radiocarbon dating. These results, when integrated with terrestrial paleoseismic data, will help us resolve the degree to which the GSL acts as a Wasatch Front lacustrine seismograph.

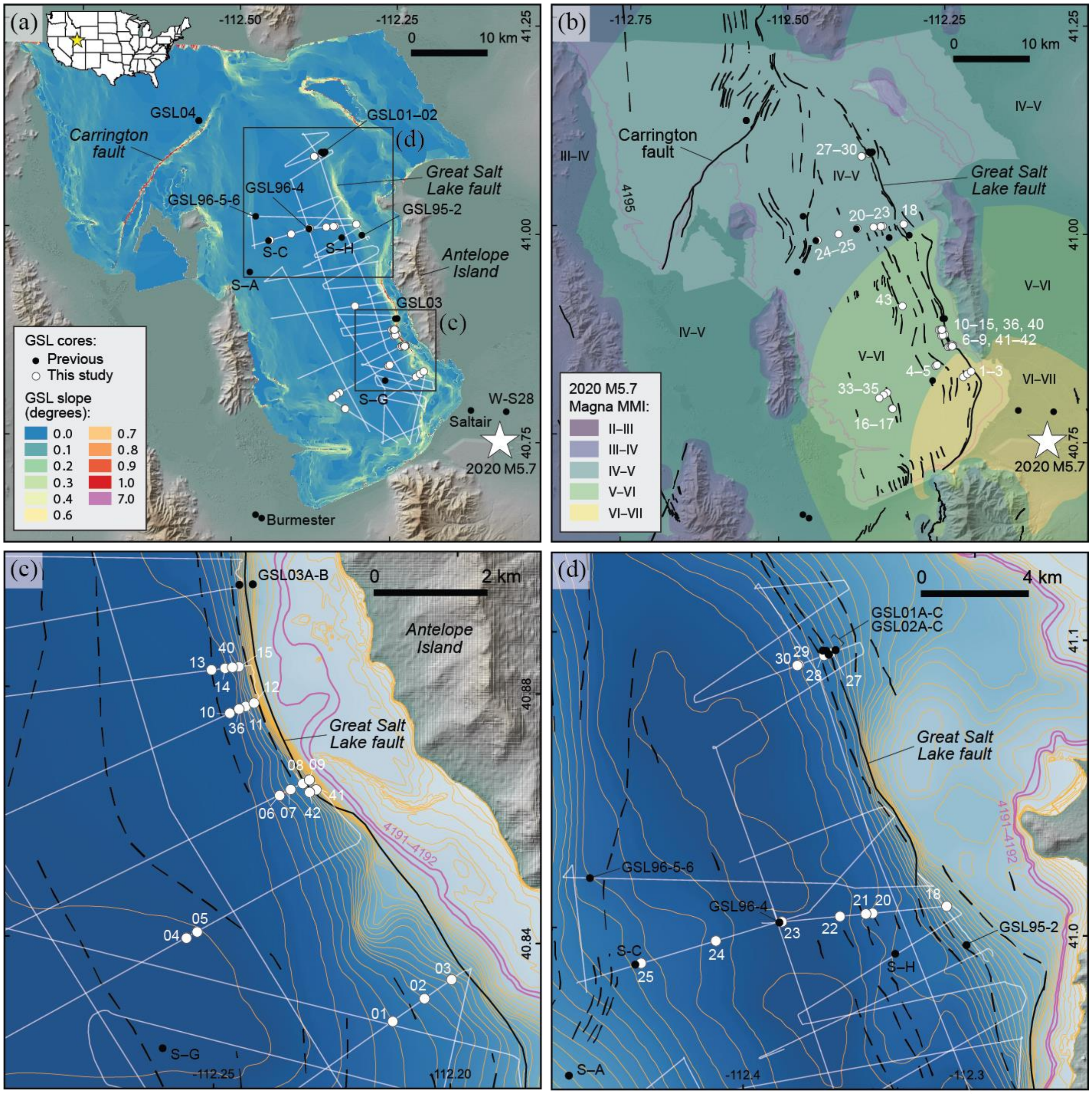

Figure 1. *Seismic-reflection surveys and sediment cores in the south arm of the Great Salt Lake, Utah. (a) Chirp track lines (white lines; this study), previous piston core locations (Spencer and others, 1984; Dinter and Pechmann, 2005; Oviatt and others, 2015), and hammer cores (this study); basemap is slope map derived from 1-foot bathymetric contours (Baskin and Allen, 2005), which highlights the Great Salt Lake and Carrington faults. (b) Hammer core locations compared to ShakeMap-derived shaking intensities for the 2020 M5.7 Magna earthquake; fault traces from Utah Geological Survey (2021). Pink line shows 4195 ft shoreline at the time of the earthquake (March 2020). (c) Hammer-core transects across the Great Salt Lake fault scarp near the southern portion of Antelope Island. (d) Piston and hammer cores northwest of Antelope Island. Pink lines show shoreline elevation at the time of this study (June–July 2021).*

References

Baskin, R.L., and Allen, D.V., 2005, Bathymetric map of the south part of Great Salt Lake, Utah, 2005: U.S. Geological Survey Scientific Investigations Map 2894, 1 p.

Dinter, D.A., and Pechmann, J.C., 2005, Segmentation and Holocene displacement history of the Great Salt Lake fault, Utah, *in* Lund, W.R., editor, Basin and Range Province Seismic Hazards Summit II: Basin and Range Province Seismic Hazards Summit II: Utah Geological Survey Miscellaneous Publication 05-2, p. 82–86.

Oviatt, C.G., Madsen, D.B., Miller, D.M., Thompson, R.S., and McGeehin, J.P., 2015, Early Holocene Great Salt Lake, USA: Quaternary Research, v. 84, no. 1, p. 57–68.

Spencer, R.J., Baedecker, M.J., Eugster, H.P., Forester, R.M., Goldhaber, M.B., Jones, B.F., Kelts, K., McKenzie, J., Madsen, D.B., Rettig, S.L., et al., 1984, Great Salt Lake and precursors, Utah: the last 30,000 years: Contributions to Mineralogy and Petrology, v. 86, p. 321–334.

Utah Geological Survey, 2021, Utah Quaternary fault and fold map, https://geology.utah.gov/apps/qfaults/ accessed November 2021.

RUPTURE IN THE MINA DEFLECTION: ACTIVATION OF THE FULL RANGE OF TRANSTENSIONAL FAULTS DURING THE 2020 MONTE CRISTO RANGE EARTHQUAKE SEQUENCE

Austin Elliott, U.S. Geological Survey, Moffett Field, CA, ajelliott@usgs.gov
Seth Dee, Nevada Bureau of Mines and Geology, sdee@unr.edu
Rich Koehler, Nevada Bureau of Mines and Geology, rkoehler@unr.edu
Ian Pierce, University of Oxford, ian.pierce@earth.ox.ac.uk
Alex Hatem, U.S. Geological Survey, Golden, CO, ahatem@usgs.gov
Christine Ruhl, University of Tulsa, cruhl@utulsa.edu
Xiaohua Xu, University of Texas, Austin, xiaohua.xu@austin.utexas.edu

ABSTRACT

An array of east-west-striking left-lateral faults transfer transtensional strain from the southern to the central Walker Lane through the Mina Deflection, a ~5,000 km^2 area east of the Mono Basin where active faulting is predominantly conjugate to the main northwest-striking right-lateral shear zone, the Walker Lane. The numerous and relatively short faults within the Mina Deflection suggest smaller maximum magnitudes compared to those possible along the relatively longer adjacent strike-slip faults in the region. However, it has been unclear how individual earthquake ruptures traverse this zone. The May 15, 2020 M_w6.5 earthquake centered in the Monte Cristo Range (MCR) south of Mina, NV ruptured faults within the Mina Deflection and illuminates how individual earthquake ruptures traverse structurally complex systems such as the Mina Deflection. Integration of observed surface rupture from the field, large-scale deformation from geodesy, and 3D fault geometry from aftershock seismicity reveals that the 2020 MCR earthquake activated left-lateral, right-lateral, normal, and oblique transtensional faults, which represent nearly the full gamut of fault types that comprise the Mina Deflection. The mainshock predominantly ruptured a buried east-west left-lateral fault, apparently the eastward continuation of the mapped Candelaria fault, which experienced only centimeter-scale slip where it was previously recognized at the surface in the west. In the epicentral zone, where left-lateral slip is confined to depths greater than 2 km, north-striking right-normal faults in the overlying alluvial and volcanic deposits show minor slip along reaches above the greatest left-lateral shear below. The largest aftershocks occurred along the conjugate right-lateral Petrified Springs fault located at the eastern end of the rupture. To the west, the mainshock ruptured a pair of oblique left-normal faults that strike more northeasterly, as well as north-south normal faults that connect them. The collection of structures that slipped during this earthquake represent the full range of transtensional fault kinematics present in the Mina Deflection, illuminate subsurface structure, and illustrate how ruptures may navigate among variously oriented smaller faults to produce relatively large-magnitude earthquakes.

PRELIMINARY ANALYSIS OF EARTHQUAKE GEOLOGY INPUT DATA FOR THE U.S. NATIONAL SEISMIC HAZARD MODEL 2023 UPDATE

Alex Hatem, U.S. Geological Survey, Geologic Hazards Science Center, ahatem@usgs.gov
Rich Briggs, U.S. Geological Survey, Geologic Hazards Science Center, rbriggs@usgs.gov
Ryan Gold, U.S. Geological Survey, Geologic Hazards Science Center, rgold@usgs.gov
Camille Collett, U.S. Geological Survey, Geologic Hazards Science Center, ccollett@usgs.gov

ABSTRACT

The USGS plans to release the next update to the U.S. National Seismic Hazard Model (NSHM) in 2023. Here, we describe revisions to the NSHM Fault Sections Database (FSD) and the geologic slip rate database (EQGeoDB) specific to the Intermountain West (IMW). The number of faults included in the FSD across the IMW increased from ~230 fault sections in previous models to ~550 fault sections in 2023 (~140% increase). The increase in the number of faults in the FSD primarily results from relaxing the previous requirement that only faults with direct measurements or estimates of slip rate be included in the NSHM (Fig. 1A & B). Where slip rates are not available from the literature, we determined a preferred rate within the Quaternary Fault and Fold Database (QFFD) slip rate bin for a given fault, in conjunction with additional guiding data (e.g., the geodetic strain rate field). These estimated rates, along with field based geologic slip rates, constitute the framework of the geologic deformation model. The EQGeoDB includes over 200 slip rate estimates within the IMW region. Partnerships between USGS and State geological surveys ensured that all available published data were incorporated into the databases.

Preliminary testing of the geologic deformation model shows that, despite adding ~200 fault sections, sub-regions within the IMW exhibit ~ 10—20% off-fault deformation when comparing geologic and geodetic moment rates within tectonic sub-regions. Fault length across the IMW increased by ~40%, but most of the newly added fault sections have an assigned slip rate of < 0.1 mm/yr. Because the update consisted primarily of short and slow faults compared to previous NSHMs, the total moment summed across the IMW only marginally increased. Rupture rates of earthquakes along individual fault sections show the highest rates of recurrence within the Walker Lane and Wasatch regions, similar to previous NSHMs, with longer rates of recurrence in lower strain regions such as the central Basin and Range Province and Rio Grande Rift (Fig. 1C). This update includes a more complete representation of Quaternary active faults across the IMW; while the aggregate increase in moment rate may be small, site-specific calculations of shaking and hazard curve disaggregations may be influenced by the incorporation of additional fault sources.

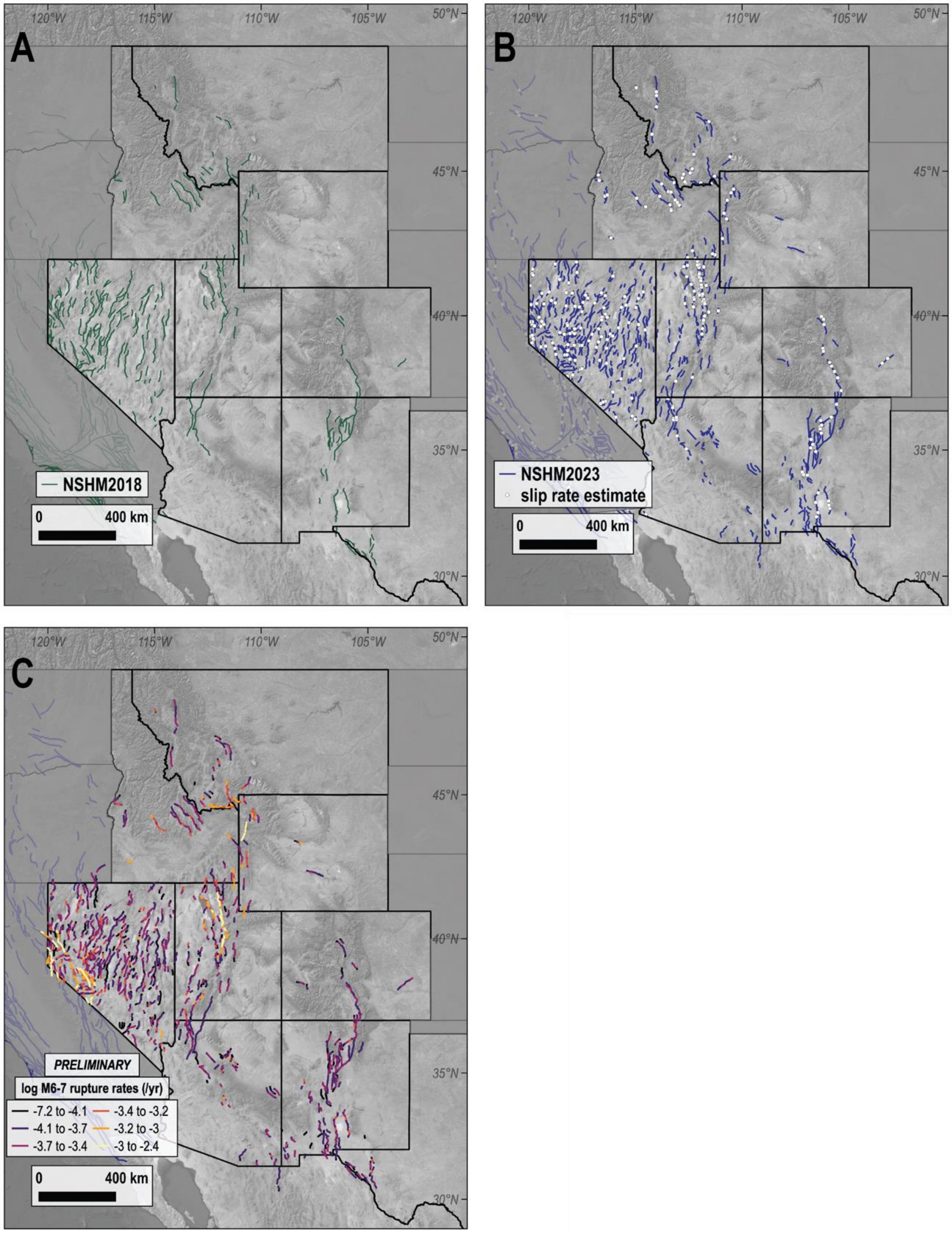

Figure 1. *NSHM Earthquake Geology input data and preliminary rupture rate testing result within the Intermountain West (IMW). (A) NSHM2018 fault sections. (B) NSHM2023 fault sections and point locations of slip rate estimates. (C) Preliminary testing results of log rupture rates (rupture magnitude ranges from 6 to 7) within a segmented model. Testing conducted in OpenSHA-fault-system-tools (Milner, 2021).*

GEOLOGIC EVIDENCE OF EARTHQUAKE BEHAVIOR ON THE EASTERN EDGE OF THE BASIN AND RANGE

Suzanne Hecker, U.S. Geological Survey, shecker@usgs.gov
David P. Schwartz, U.S. Geological Survey, dschwartz@usgs.gov
Timothy E. Dawson, California Geological Survey, Timothy.Dawson@conservation.ca.gov

ABSTRACT

Paleoseismic and historical observations from the Rocky Mountains provide clues into the source and timing characteristics of large normal-faulting earthquakes along the eastern margin of Basin and Range extension. From a survey of maximum vertical displacements for latest Quaternary and historical surface ruptures, we have found that the ratio of fault slip to fault length, an indicator of static stress drop, is generally largest for structurally immature faults, those with the smallest cumulative displacements (<2 km; Hecker et al., BSSA, 2010). Immature faults are relatively common in the Rocky Mountain region, and their tendency to produce larger-stress-drop earthquakes may reflect greater strength-related roughness and geometric complexity. A recent investigation into the paleoearthquake history of one such fault, the Holocene-activated Bear River fault zone in Wyoming and Utah, yielded age constraints for the initial two events on the fault that fall within a previously recognized mid- to late Holocene cluster of earthquakes in the southern Middle Rocky Mountains (Hecker et al., Tectonophysics, 2021). This period of elevated strain release on and between widely spaced, low-slip-rate faults, and in particular the apparent close timing of events on the Bear River fault zone and its nearest neighbor, the Rock Creek fault, suggests interrelated fault activity arising from a regionwide redistribution of stress or other perturbation of the stress field. Clustering among networks of similar-slip-rate faults has been interpreted as indicating a strong tendency toward synchronization of seismic cycles and has been recognized elsewhere in intraplate settings, such as for historical and prehistoric earthquake sequences in the central Nevada seismic belt (Scholz, BSSA, 2010). The implications for regional seismic hazard of space-time clustering of high-stress-drop earthquakes are that damaging earthquakes may occur more frequently (or less, depending on where we are situated in the seismic cycle) than indicated by long-term average recurrence estimates and with stronger high-frequency ground motion than may be inferred using general magnitude-fault-length scaling relations. These results point to the need for paleoseismic investigations aimed at characterizing regional fault-group behavior (including possible propensity for high stress-drop earthquakes) and for incorporating the effects of earthquake clustering in time-dependent probabilistic seismic hazard assessments.

DETAILED QUATERNARY FAULT-TRACE MAPPING OF THE WASHINGTON, HURRICANE, AND SEVIER/TOROWEAP FAULT ZONES IN UTAH AND ARIZONA

Tyler R. Knudsen, Utah Geological Survey, tylerknudsen@utah.gov
Adam I. Hiscock, Utah Geological Survey, adamhiscock@utah.gov
Jeri Ben-Horin, Arizona Geological Survey, jeribenhorin@arizona.edu
Philip A. Pearthree, Arizona Geological Survey, pearthre@arizona.edu

ABSTRACT

The Utah Geological Survey (UGS) and the Arizona Geological Survey (AZGS), with support from the U.S. Geological Survey External Grants Program, completed lidar-based Quaternary fault-trace mapping of the Hurricane, Washington, and Sevier/Toroweap fault zones in southwestern Utah and northeastern Arizona. Where permissible with available lidar coverage, we mapped additional faults adjacent to and possibly structurally related to the Hurricane fault zone, including the Enoch graben, Parowan Valley, and Paragonah faults. These faults pose a significant earthquake hazard to this rapidly urbanizing area of the southwest U.S. In addition to lidar-derived imagery, we used existing geologic mapping, paleoseismic investigations, historical aerial photography, and field investigations to map surface fault traces and to locate scarps amenable to paleoseismic trenching investigations. In Utah, the UGS delineated special-study areas around each fault to encourage recognition, additional investigation, and mitigation of hazardous faults for infrastructure and development. We identified 72 potential trenching sites that may be further evaluated for paleoseismic investigations. Significant discoveries made during our mapping include: (1) some Parowan Valley fault scarps have formed on late Holocene stream alluvium and playa deposits, and likely represent the youngest surface ruptures known in southwest Utah; (2) surface-rupture recency of some Enoch graben faults is obscured where faults exhibit evidence of both seismogenic Holocene surface rupture and aseismic historical creep due to aquifer compaction and ground subsidence related to groundwater mining; (3) the most youthful-appearing scarp (late Pleistocene to Holocene) identified on the main trace of the Sevier/Toroweap fault is superimposed on a significantly older, well-developed obsequent fault scarp, indicating that the average recurrence interval between surface-faulting earthquakes on the Sevier/Toroweap fault in Utah may be relatively long (several tens of thousands of years). Fault-trace geometries and attributes will be published to the UGS *Utah Geologic Hazards Portal*, the AZGS active fault theme on the *Natural Hazards in Arizona Viewer*, and shared with the U.S. Geological Survey for updating the *Quaternary Fault and Fold Database of the United States*.

QUATERNARY FAULT COMPILATION FOR THE INGENIOUS GEOTHERMAL PROJECT

Rich Koehler, University of Nevada, Reno, Nevada Bureau of Mines and Geology, rkoehler@unr.edu
Zachery M. Lifton, Idaho Geological Survey, zlifton@uidaho.edu
Emily J. Kleber, Utah Geological Survey, ekleber@utah.gov
Tyler Knudsen, Utah Geological Survey, tylerknudsen@utah.gov
Adam Hiscock, Utah Geological Survey, ahiscock@utah.gov
Stefan Kirby, Utah Geological Survey, stefankirby@utah.gov
Craig dePolo, University of Nevada, Reno, Nevada Bureau of Mines and Geology, cdepolo@unr.edu
James Faulds, Nevada Bureau of Mines and Geology, jfaulds@unr.edu
Bridget Ayling, Nevada Bureau of Mines and Geology, bayling@unr.edu

ABSTRACT

Thin continental crust, active normal faults, volcanic centers, and permeable rocks make areas of the Great Basin ripe for geothermal potential and production. The U.S. Department of Energy-funded collaborative INnovative Geothermal Exploration through Novel Investigations Of Undiscovered Systems (INGENIOUS) project aims to reduce the exploration risk for hidden geothermal systems in the Basin and Range Province to enhance the understanding of geothermal potential and increase private investment in geothermal energy. As part of the INGENIOUS team, the Nevada Bureau of Mines and Geology, Utah Geological Survey, and Idaho Geological Survey have compiled initial databases for Quaternary faults, seismicity, volcanic deposits, and other relevant information for inclusion in the analysis. Certain structural settings where Quaternary faulting occurs can indicate local permeability and geothermal potential, and therefore fault mapping and rupture parameter data (i.e., slip rates and recency of movement) are important to the project. The INGENIOUS fault database is based on information contained in the *U.S. Quaternary Fault and Fold Database* and individual state fault databases, which contain fault names, mapped scale, slip sense, dip direction, binned categories for slip rate, and age of most recent movement. Starting with these databases, additional data was added, including more discrete ages of the last movement, as well as geologic slip-rate information from published literature. Preferred slip rates developed for the earthquake geology inputs to the 2023 update of the U.S. National Seismic Hazard Model (NSHM) (Hatem et al., 2022) were applied where available. For faults that had no data related to recency of movement and/or slip rate, we used geological observations based on the relative age of geomorphic deposits, fault scarp geomorphology, amount of displacement, and other factors to evaluate these parameters. We will present an updated database of faults, including the recency of faulting and slip rate data, as well as additional fault geometries.

INSIGHTS INTO SEGMENTATION OF THE OQUIRRH – GREAT SALT LAKE FAULT SYSTEM FROM FAULT SCARP HEIGHTS AND LAKE BONNEVILLE SHORELINE ELEVATIONS

Charles F. Memmott, Utah Valley University, cfmemmott6@gmail.com
Michael P. Bunds, Utah Valley University, michael.bunds@uvu.edu

ABSTRACT

The Great Salt Lake Fault (GSLF), North Oquirrh Fault (NOF), South Oquirrh Fault (SOF), and Topliff Hills Fault (THF) form a >200 km long, range-bounding, west dipping fault system in the eastern Basin and Range near the populous Wasatch Front. The GSLF appears to connect at its south end to NOF, but it is submerged beneath the Great Salt Lake and detail of the structural connection of the two faults is unclear. The NOF and SOF are separated by a structural complexity that obscures their linkage, although tentatively identified fault scarps in the complexity may provide insights. Age constraints for the most recent event (MRE) on each of the four faults are permissive of co-rupture, although age overlap for the NOF and SOF is small and MRE timing on the GSLF and THF are not well known (MRE ages are: GSLF post 10 ka (Dinter & Pechmann, 2014), NOF 4.8 – 7.9 ka (Olig et al., 1996), SOF 1.3 – 4.8 ka (Olig et al., 2001), and THF post 12.8 ka (Ward et al., 2019)). We investigate segmentation behavior between the NOF and GSLF, and between the NOF and SOF using the along-strike distribution of surface offset in the MRE and earlier surface-rupturing earthquakes, combined with the elevation of Lake Bonneville shorelines that parallel the NOF and were displaced by surface faulting. 220 measurements of net vertical displacement (offset) were made along the scarps of the NOF and SOF using LiDAR digital topography. Our preliminary results show that total offset across fault scarps fall into three groups: one-event offsets that range from 2 to 3 m, two-event offsets that range from 5 to 7 m, and three or more event offsets that range from 7 to 10.5 m. One event scarp heights are consistent with trenching results (Olig et al., 1996) and are restricted to sections of fault that displace Bonneville sediments. MRE offset on the NOF increases northward from ~2.4 m in the central portion of the fault to ~3.4 m at its north end near where it connects to the GSLF. A pooled T-test at 95% confidence indicates that this upward trend to the north is statistically significant. This suggests that the MRE on the NOF may have included rupture on at least the southern part of the GSLF, consistent with an estimated >40 km rupture length of the MRE based on offset (Wells and Coppersmith, 1994, Olig et al., 2001) if the rupture terminated to the south at the south end of the NOF (Bunds et al., 2016). Lake Bonneville shorelines in the NOF footwall, which pre-date the MRE and post-date the penultimate event (PE), increase in elevation to the north supporting this hypothesis, although it is difficult to separate isostatic rebound from tectonic effects on shoreline elevation. In contrast, preliminary results indicate that offset in the PE may decrease towards the north end of the NOF, suggestive of a different rupture distribution in that event. Ongoing work includes analysis of offset along the southern NOF and SOF to address segmentation between those faults.

Paleoseismic History of the Genola North Fault at the West Mountain Site and connectivity with Utah Lake Faults

Kristen E. Smith[1]*, Nathan A. Toké[1], David R. Johnson[1], Charles Doug Czajka[1], Daren T. Nelson[1], Adam I. Hiscock[2]

[1]Utah Valley University [2]Utah Geological Survey *krstnwolf92@gmail.com

ABSTRACT

Lidar analysis has led to the discovery of many previously unrecognized active faults, including a 13-km-long discontinuous network of fault scarps running along the west side of West Mountain in Utah County. This westward dipping normal fault, called the Genola North fault, aligns with the Lincoln Point West fault system, within Utah Lake, as well as the Long Ridge fault, located to the south. These faults have been postulated to be coseismic, auxiliary faults to the Provo segment of the Wasatch fault zone. If linked together, these three faults comprise an approximately 40-km-long fault system. Characterizing their seismic hazard is an important consideration for urban development along West Mountain and on Utah Lake. Based upon our lidar interpretation, we selected the West Mountain site (40.1148, -111.8406) due to a ~ 3-m high fault scarp cutting the Provo shoreline of Lake Bonneville along the northern half of West Mountain. This site is ideal for paleoseismic analysis because of the known geomorphic age for the Provo level shoreline of Lake Bonneville (~ 15 cal ka). A single 30-m-long trench across the fault scarp revealed 20° westward dipping transgressive and regressive lake deposits below a prominent angular unconformity marked by a near horizontal ~ 10-cm thick carbonate beach deposit. The displacement of the carbonate beach deposit shows a 5-m organic soil-filled fault zone with 3-m of vertical movement. We also observed clear evidence of two ground rupturing earthquakes post Lake Bonneville and at least one rupture close in time to the Bonneville highstand (~18 cal ka). Based on these shoreline ages, we infer an average recurrence rate of 7.5 ka per event and a slip rate of ~0.2 mm/a. Freshwater mollusk shells common to Bonneville basin were sampled for C-14 dating and amino acid racemization to provide age range of the transgressive and regressive lake deposits. Bulk soil samples from fault-derived colluvium should provide additional C-14 dates to help constrain the timing of the penultimate earthquake and the maximum age of the most recent event. Two optically stimulated luminescence (OSL) samples were also collected to help support the radiocarbon dating samples. Other funding is needed to process these OSL samples. This study provides evidence that faults along West Mountain have been active within the Holocene and should be taken into consideration for urban planning in this rapidly growing region.

Lidar Data Reveal Evidence for Late Quaternary Faulting 5km East and nearly 1000 m above the Bonneville High Stand, Cutting Glacial Moraines and Talus Cones of the Timpanogos Massif Along the Northern Provo Segment of the Wasatch Fault

Authors: Nathan A. Toké, David Johnson, and Kristen Smith

Utah Valley University

Documenting fault zone width is necessary for characterizing key fault parameters such as slip-rate and earthquake recurrence. The 2014 State of Utah lidar data acquisition provided crucial data for understanding the locations of fault surface rupture hazard along the urban corridor and piedmont of the Wasatch Front; however, the dataset did not span the full width of the Wasatch fault zone. The 2018 Central Utah lidar data demonstrates the importance of collecting wider aperture high resolution topography to fully document fault systems such as the Wasatch. Using lidar derived slopeshade and aspect maps, we identified convincing evidence for fault scarps with multi-meter surface displacements along the high geomorphic features below the west facing cliffs of the Mount Timpanogos massif. Fault surface displacements vary in magnitude with the ages of the geomorphic features that are displaced. Young debris cones are displaced by 2-3 m, recent glacial moraines appear to be displaced by more than 5 m, and older talus cones have displacements ranging from 10 m to more than 20 m. Fault surface breaks extend discontinuously along the massif for at least 10 km and individual fault traces range from ~ 200 m to more than 1500 m in length. The high fault traces are primarily located within the Bridal Veil Limestone member of the Oquirrh Formation and some faults crop out within the Manning Canyon Shale. Our mapping along the northern Provo segment, demonstrates that the surface trace of the Wasatch fault extends across a ~5km-wide zone extending from near the Bonneville shoreline to the base of the high cliffs of Mount Timpanogos, nearly 1000 meters above the piedmont. The full distribution of fault surface traces between the piedmont and the cliff face is challenging to map due to the presence of numerous landslides within the Manning Canyon Shale and across the fault zone.

LIDAR DATA REVEAL NEW FAULTS IN THE EPICENTRAL REGION OF THE 2020 M6.5 STANLEY, IDAHO EARTHQUAKE

Mark S. Zellman, mzellman@bgcengineering.com
Zachery M. Lifton, zlifton@uidaho.edu
Christopher B. DuRoss, cduross@usgs.gov
Glenn D. Thackray, glennthackray@isu.edu

ABSTRACT

The 31 March 2020 M6.5 Stanley earthquake occurred in central Idaho, within the Centennial Tectonic Belt, which includes the Basin and Range Province extension north of the Snake River Plain. The earthquake is enigmatic because it occurred ~18 km north-northeast of the Holocene-active Sawtooth fault in an area devoid of Quaternary-active structures and yielded focal mechanisms with north-south or east-west dominantly lateral slip rather than normal faulting. Aftershocks form a north-northwest-oriented alignment; although they continue south to the central portion of the Sawtooth fault, they are dominantly in the footwall of this east-dipping structure. These observations indicate that seismogenic structures in this part of central Idaho are more complex than current mapping suggests.

We use high-resolution (QL1) post-event lidar data to characterize potentially seismogenic structures in the Stanley earthquake epicentral region. The post-event lidar is part of a regional collection area for central Idaho that includes the entire Sawtooth fault. Here, we focus on geomorphic mapping at the northern end of the Sawtooth fault and within the Stanley earthquake epicentral region. Our preliminary mapping reveals that the northern Sawtooth fault is complex. The fault includes a ~10-km-long north-eastern splay that diverges from the range-front fault at a 10º angle, and the main fault extends at least 6 km farther to the north than previously mapped. About 5 km west of the Sawtooth fault, we mapped a 10-km-long northwest-trending linear alignment of fault scarps that displace late Pleistocene glacial and alluvial deposits and apparently crosscut the northeast trending Trans-Challis fault system at a 30º angle. West-facing scarps imply a west-dipping fault, in contrast to the east-dipping Sawtooth fault. The fault scarps cross a broad valley floor and are aligned with a linear valley that extends to the south. To the north, the scarps climb topography before becoming indistinct on ridgetops in steep glaciated terrain. Because this previously unrecognized Quaternary-active structure is generally west of the north-south-aligned Stanley earthquake aftershock zone, its relation to the source of the 2020 mainshock is unclear.

Geology - Monday October 17

Session Conveners: Alex Hatem (U.S. Geological Survey), Rich Koehler (Nevada Bureau of Mines and Geology), and Zach Lifton (Idaho Geological Survey)

Extended Abstracts:

Genevieve Atwood	Earth Science Education	Basin and Range shorelines: Historians of climate, geomorphic, and tectonic change

BASIN AND RANGE SHORELINES: HISTORIANS OF CLIMATE, GEOMORPHIC, AND TECTONIC CHANGE

Genevieve Atwood, Earth Science Education, genevieveatwood@comcast.net
Natalie A. Hilker, Earth Science Education, nataliehilker@me.com
Tamara Wambeam, wambeam@comcast.net

ABSTRACT

From G.K. Gilbert to the present, Earth scientists have recognized shoreline evidence as storehouses of Earth process information. For open-basin lakes of the Basin and Range, such as paleo-Lake Bonneville or modern Utah Lake, the elevation of the threshold outlet essentially controls the elevation of that lake's shoreline evidence. A lake's threshold is the low place on the basin's rim where a lake crosses into another basin.

Northwestern Utah has many basins, many faults, and ample opportunity to study patterns of shoreline evidence as the interplay of erosion/deposition and tectonics. Interpreting the shoreline evidence of paleolakes may contribute to understanding the tectonics of the Basin and Range.

Patterns of shorelines include series of younger vs. older evidence and progressively higher vs. lower evidence. When threshold elevation lowers, the lake's younger shorelines are lower. When the threshold rises, the younger shorelines are higher. When portions of the floor of the lake drop (basin depresses), the lake level drops and then recovers to its threshold level. The younger shorelines are higher than the older. For that reason, already-identified series of upward-ramping, upward-younger shoreline series may contribute to an understanding of Basin and Range tectonics and lake-level history.

Figures:

Figure 1: Location map, Lake Bonneville, Red Rock Pass, Great Salt Lake, and Utah Lake.
Figure 2: Scenario 1. Lower the threshold.
Figure 3: Scenario 2. Raise the threshold.
Figure 4: Scenario 3. Basin extension.

FIGURES

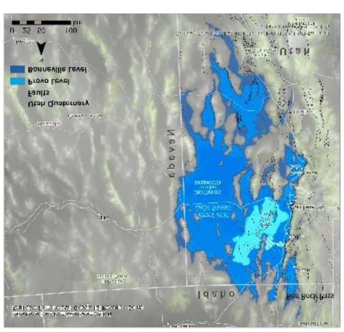

Figure 1. Location map.

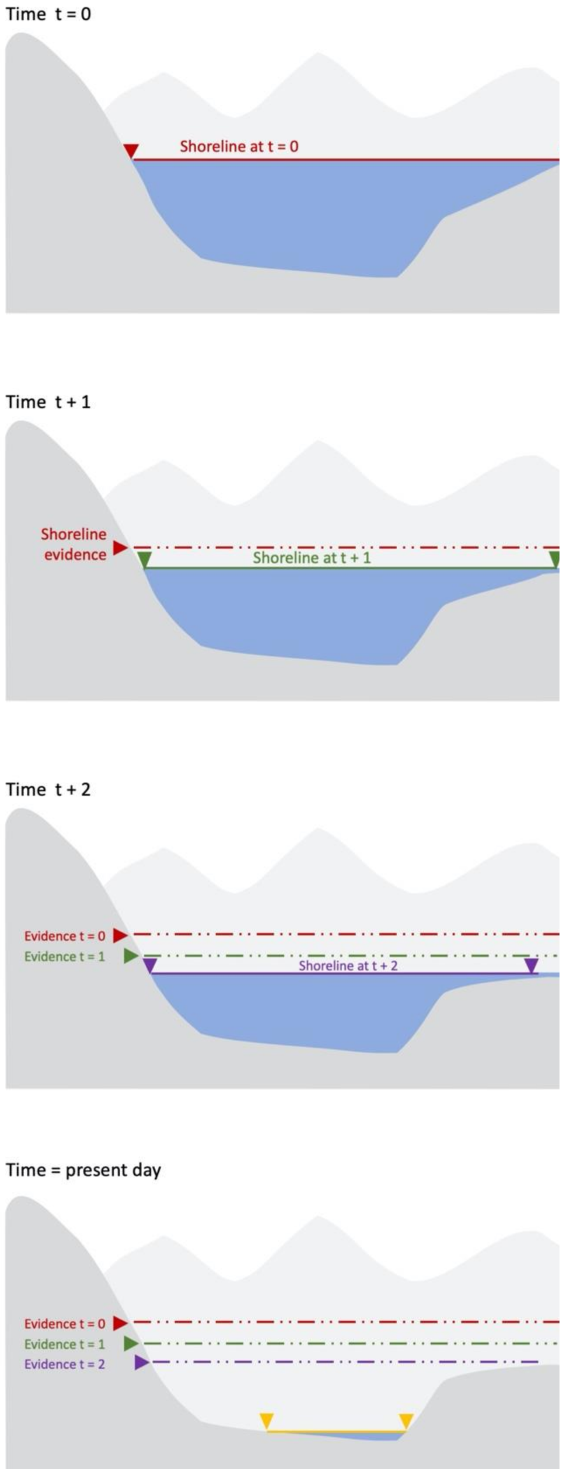

Figure 2. Scenario 1. Lower the threshold. In scenario one, as a lake's threshold erodes, the lake level drops, leaving a pattern of younger, lower shoreline evidence (see figure 2). The erosion could be caused by a catastrophic event such as the Bonneville flood at Red Rock, ID or in a slower, steadier, continuous erosional process

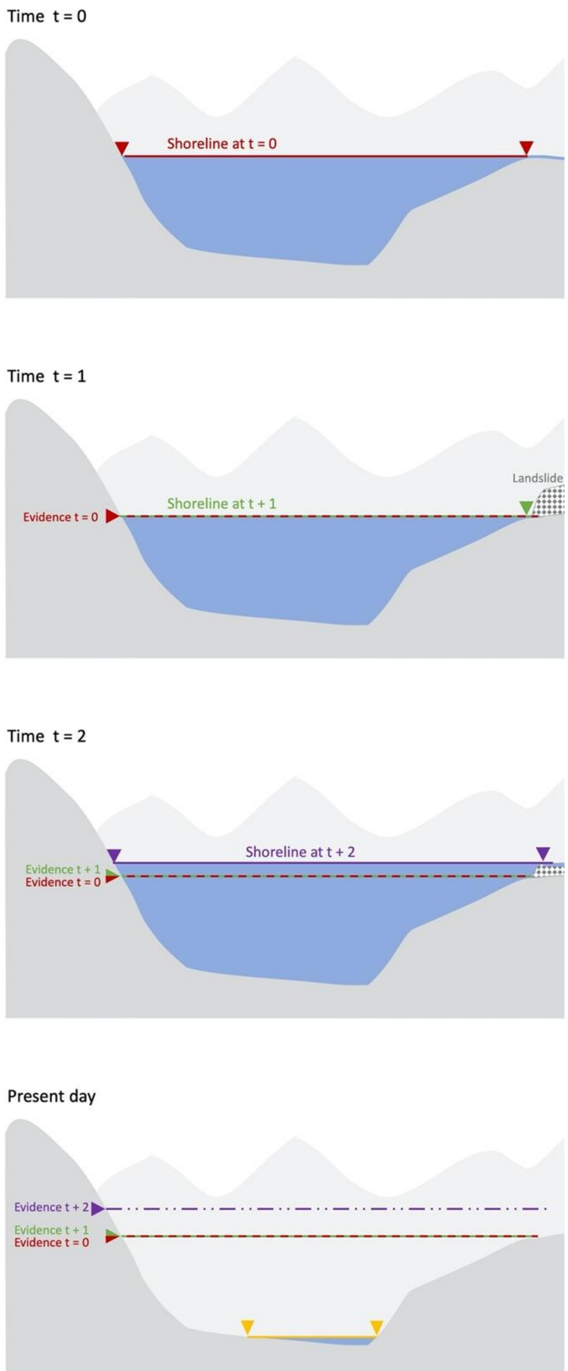

Figure 3. Scenario 2. Raise the threshold.
In scenario two, as the lake's threshold rises, the lake level rises, leaving a pattern of younger higher shoreline evidence. The rise of threshold elevation could be caused by a geomorphic processes, such as a landslide blocking the outlet, or due to tectonic uplift, creating younger, higher shoreline evidence.

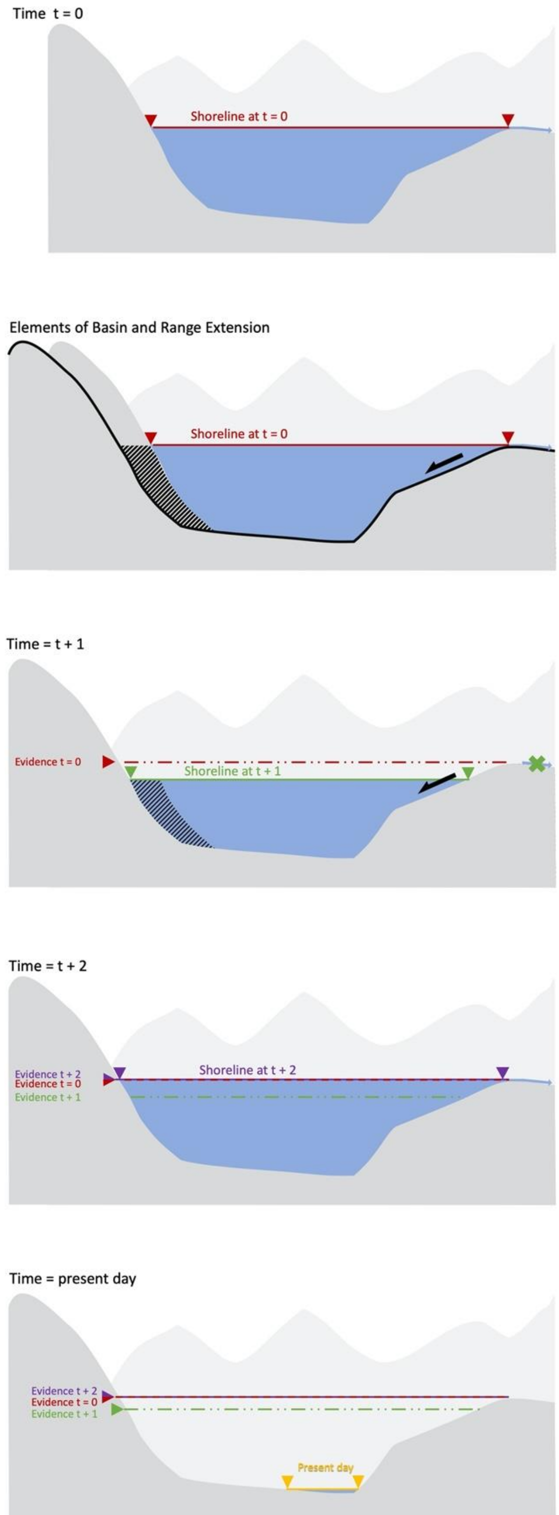

Figure 4. Scenario 3. Basin extension.
In scenario three, the threshold remains steady. Basin and Range extension increases the volume of the lake's basin. Lake level immediately drops below the threshold. The closed-basin lake rises in response to climate until becomes an open-basin lake overflowing (again) at the threshold. As lake-level rises, it may leave a complex, but generally rising series of younger shorelines between the evidence of t + 1 and t + 2. At t + 2 the lake is a threshold-controlled open basin. Basin extension, creates younger, higher shoreline evidence. This may feel counter intuitive. Patterns of Scenario 3 caused by tectonics resemble those of Scenario 2 caused by geomorphic processes.